01 Aug 2000

FDTD and FEM/MOM Modeling of EMI Resulting from a Trace Near a PCB Edge

Daniel P. Berg

Motoshi Tanaka

Yun Ji

Xiaoning Ye

et. al. For a complete list of authors, see https://scholarsmine.mst.edu/ele_comeng_facwork/1628

Recommended Citation

D. P. Berg et al., "FDTD and FEM/MOM Modeling of EMI Resulting from a Trace Near a PCB Edge," *Proceedings of the IEEE International Symposium on Electromagnetic Compatibility (2000, Washington, D.C.)*, vol. 1, pp. 135-140, Institute of Electrical and Electronics Engineers (IEEE), Aug 2000.
The definitive version is available at https://doi.org/10.1109/ISEMC.2000.875551

FDTD and FEM/MOM Modeling of EMI Resulting from a Trace Near a PCB Edge

D. Berg, M. Tanaka*, Y. Ji, X. Ye, J. L. Drewniak, T. H. Hubing, R. E. DuBroff, and T. P. Van Doren
Electromagnetic Compatibility Laboratory
Department of Electrical and Computer Engineering
University of Missouri-Rolla
Rolla, MO 65409-0040
*Faculty of Engineering and Resource Science
Akita University
Akita, Japan

Abstract: PCB traces routed near board edges and carrying high-speed signals are considered to contribute to EMI problems. Consequently, design maxims state that traces that might have intendtional or unintentional high frequency components on them be kept away from board edges. This costs valuable surface area as boards become more densely designed. Further, design maxims concerning tracesnear board edges are not well quantified. The increase in EMI as a trace is routed increasingly closer to the PCB edge has been studied experimentally and with numerical modeling.

1. INTRODUCTION

A common maxim for printed circuit design is to maintain high-speed traces interior to the PCB, where a "keep-out" area is designated near the board periphery. This design maxim might be motivated by a number of factors, but can include impedance control, and EMI. The design maxim is typically specified by designating that the high-speed trace is kept a given number of heights of the PCB trace above the signal return plane away from the board edge. For example, if h is the height of the PCB trace above the ground plane, and d is the distance of the trace from the board edge, then d/h might be specified to be larger than ten or twenty. However, as design densities continue to increase, this design maxim limits routing flexibility. The present study focused on the EMI consequences of routing a trace with an intended high-speed signal, or a nominal low-speed line with unintended high-frequency components on it near the board edge. The frequency range of concern was from *100 MHz – 3 GHz.* Experimental work and numerical modeling are used to quantify this effect.

The EMI coupling physics at lower frequencies is dominated by the magnetic field. For an infinite plane, there is no magnetic flux below the plane, and, hence, all magnetic field lines wrap the signal conductor. Consequently, there is no inductance associated with the return plane [1], and in this ideal case, the impedance of the signal return is zero. However, for actual PCB designs, in which the signal return plane will have finite width, magnetic field lines close below the plane [2], [3], and the return plane will have a non-zero partial inductance [2], [4], [5], [6]. The signal return currents through this non-zero impedance leads to radiation as a result of the potential difference across the signal return, and this effective noise source driving portions of the extended reference conductors against each other [7]. Simple approximations for the current distribution in the signal return plane can be used to deduce a relationship for the resulting EMI as a function of the trace height above the ground plane, and the width of the ground plane [2], [3], [8]. This radiation results entirely from the non-zero impedance of the signal return plane. However, the associated partial inductance is still small as compared to the inductance in the signal trace for typical PCB plane widths. When the trace is sufficiently long, coupled transmission-line modeling has been used estimate the resulting EMI for a given source [9]. The assumption here is that the problem is translationally invariant, and that cross-sectional parameters can be extracted for the transmission-line modeling.

In the work presented herein, the trace is brought in proximity to the board edge. This results in increased magnetic field lines closing beneath the planes, with an expected increase in radiated fields. Also, as the height above the trace is increased, there is increased magnetic flux below the signal return plane, an increase in the signal return plane impedance, and an increase in radiation. The objective of the present study is to quantify the increase in the radiation for a signal brought near the board edge versus a signal interior to the PCB, as well as apply full-wave numerical modeling to ascertain the behavior at frequencies beyond which the static or low-frequency modeling may apply. An experimental test vehicle was constructed, and measurements made in two frequency ranges. The finite-difference time-domain modeling (FDTD) method, and a hybrid FEM/MOM approach were used to model the problem. The modeled results agreed favorably with the measurements, and provide a basis for studying the problem.

2. EXPERIMENTAL PROCEDURE AND RESULTS

Five individual test boards were constructed for the measurements. The geometry of the boards is shown in Figure 1. The boards were *10 cm* wide, and *15 cm* long. The traces were *5 cm* long and *25 mils.* wide, and had a

0-7803-5677-2/00/$10.00 ©2000 IEEE

characteristic impedance of *90 Ω*. The thickness of the FR-4 substrate was *45 mils.*, and the dielectric constant was $\varepsilon_r = 4.5$. The bottom layer of the board was a solid copper return plane. The traceand resistor bonding pads were producded with a PCB milling machine.

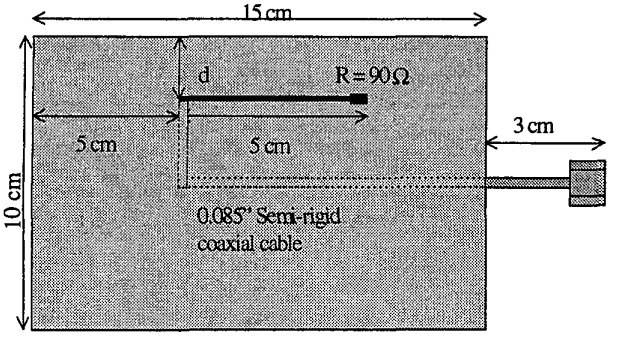

Figure 1: Geometry of PCB layout.

The distances from the edge of the board to the edge of the trace for the five test boards were *25 mils.*, *75 mils.*, *275 mils.*, *575 mils.*, and centered. Each trace was terminated with two stacked *180 Ω* resistors in parallel to make a *90 Ω* termination. The board was driven by a *0.085"* semi-rigid coax cable running along the center of the board on the underside. The cable ran the length of the board to the feed point of the driven trace, and was soldered to the ground plane along its entire length. The center conductor of the semi-rigid coaxial cable was extended beyond the outer shield and penetrated the PCB through the bottom to connect to the trace on the top side. The coaxial cable extended *3 cm* beyond the board edge and an SMA connector was located at the end of the line.

Table 1. Comparison of height above PCB reference plane and trace proximity to board edge (d).

Height (mils)	d (mils)	d/h	Termination
45	25	0.55	90 Ω
45	75	1.67	90 Ω
45	275	6.11	90 Ω
45	575	12.8	90 Ω
45	1956 (centered)	43.5	90 Ω
90	1956 (centered)	21.7	116 Ω
22	1956 (centered)	88.9	60 Ω
22	25	1.14	60 Ω

The common mode current on the outer shield of the feed cable was measured using a network analyzer. $|S_{21}|$ was measured from *100 MHz - 1 GHz* with the current probe as shown in Figure 2. Port 1 was connected to the *0.085"* coaxial cable to drive the signal line, and Port 2 was connected to a current probe (Fischer F-2000). The current probe was attached to an electrically large ground plane and circled the coaxial cable. The network analyzer was calibrated using a shorted copper ring that encircled the current probe and driven at Port 1 for the thru calibration. Then, the frequency response of the current probe was eliminated in the calibration procedure. The received voltage at Port 2 is related to the common mode current by $|V_2^-| = 50|I_{cm}|/2$. Since the source voltage is matched, the input voltage at Port 1 is $|V_1^+| = |V_s|/2$. Then, since $|S_{21}|$ is the ratio of the received voltage at Port 2 to the input voltage at Port 1, $|S_{21}| = 50I_{cm}/V_s$. The results of these measurements are shown in Figure 3. A *60 cm x 60 cm* aluminum plate was used as an electrically large ground plane to isolate the DUT from the measurement equipment and test cables. This experimental setup provided a controlled measurement environment with repeatable measurements, and also enhanced the dynamic range of the measurements.

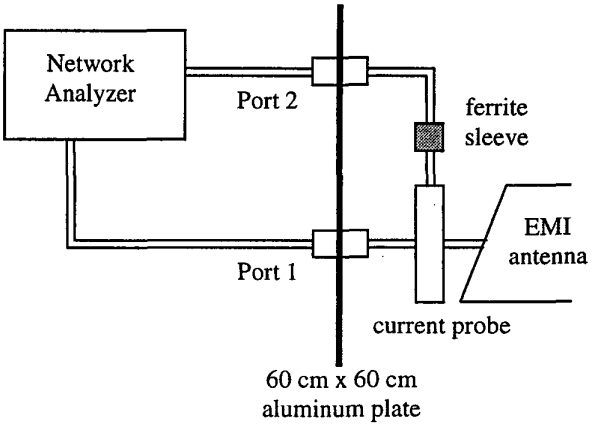

Figure 2: Test setup for measuring the $|S_{21}|$ with a current probe.

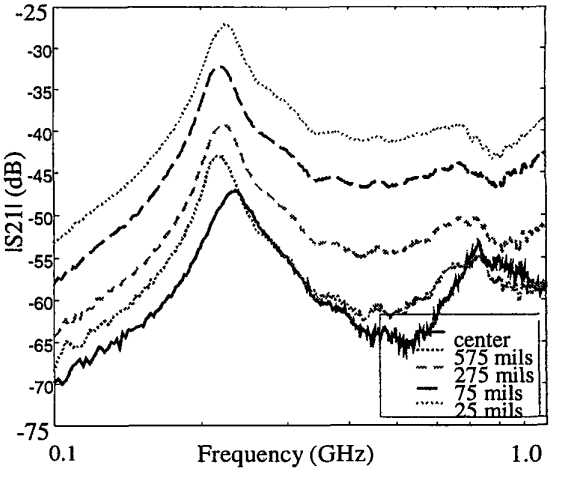

Figure 3: $|S_{21}|$ measurements with a current probe.

The second series of tests measured the near electric field from the driven board in the range *500 MHz - 3 GHz* using a monopole probe. This configuration also used the network analyzer to make $|S_{21}|$ measurements, an electrically large ground plane, and a *3 cm* monopole probe for the experimental

procedure. The setup for the experiment is identical to that in Figure 2, except the current probe was replaced with a *3 cm* long monopole probe. The two connections from the network analyzer penetrate the conducting plane through SMA feed-throughs, with a center-to-center spacing of *5 cm*. The monopole probe was centered with respect the PCB geometry. Port 1 was connected to the *0.085"* coaxial cable to drive the signal line on the test board. Port 2 was connected to the *3 cm* monopole probe.

The $|S_{21}|$ for the common-mode current results are shown in Figure 3. The resonance slightly above *100 MHz* results from the large-scale EMI antenna geometry driven against the aluminum plate. In the frequency range below the first distributed resonances, approximately *100 – 170 MHz*, the increase in the radiation with frequency is approximately *12 dB/octave*, which is consistent with a magnetic field coupling mechanism [7]. The curves are offset by a constant increase over frequency, except the centered trace as a result of a shift in resonances. This constant shift is also indicative of EMI coupling dominated by the magnetic field to *1 GHz*. The increase in the measured common-mode current is tabulated as a function of the trace proximity to the board edge in Table 2. The lower frequency portion of the curves in Figure 3 was used where the slope with frequency was *12 dB/octave*. As the trace nears the board edge, the increase is nearly *18 dB* for a trace with the edge *25 mils* away from the PCB edge.

Table 2. Increase in $|S_{21}|$ as the trace nears the PCB edge. The reference is a centered trace.

Distance from Edge (d)	$\Delta\|S_{21}\|$ (dB)
25 mils.	17.6
75 mils.	13.1
275 mils.	6.61
475 mils.	3.33

The $|S_{21}|$ results using a monopole near-field probe for each of the test boards is shown in Figure 4. The $|S_{21}|$ in the measurements is the ratio of the forward voltage on the input port to the received voltage at the monopole probe terminals. Since the feed cable and the source impedance are matched, the forward voltage is simply $\frac{1}{2} V_s$, where V_s is the source voltage. Further, the voltage induced on the monopole probe is proportional to the product of the antenna effective length and the incident electric field [10]. Then, $|S_{21}|$ in this case is proportional to the ratio of the electric field at the monopole probe, and the source voltage. Also, the monopole probe is oriented to receive a dominant polarization of the radiated field from the PCB. There are two potential radiation mechanisms for the present test configuration, radiation as a result of the non-zero impedance of the reference plane, and direct radiation from the trace. The measurement method does not allow for distinguishing between these two components. However, demonstrating a numerical modeling approach through experimental corroboration will allow for greater flexibility in distinguishing between these two radiation components. At lower frequencies as the trace is brought closer to the edge of the board, the $|S_{21}|$ increases. The measured electric field is a relatively strong function of the trace proximity to the board edge. The trace is approximately $\frac{1}{2}\ \lambda$ long at *1.5 GHz* on the FR-4 substrate. At the higher frequencies, direct radiation from the trace may be more significant relative to the radiation due to the non-zero impedance of the signal return plane, and, hence, a decreasing dependence of the radiation on the proximity of the trace to the board edge. This conjecture requires further work, and continuing numerical modeling will be used to ascertain the radiation mechanisms. Also, as the frequency increases, the trace is becoming electrically longer in terms of wavelengths. It is clear from the measurements, however, that the radiation at higher frequencies is a much weaker function of the proximity of the trace to the board edge.

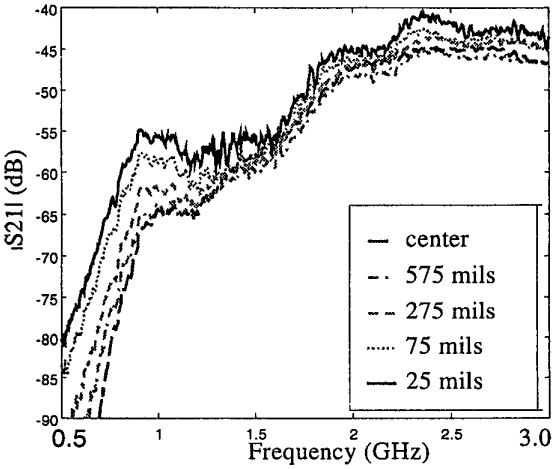

Figure 4: $|S_{21}|$ measurements using a 3 cm monopole probe.

3. Numerical Modeling of a Trace Near PCB Edges

Previously, the mixed scale dimensions of a trace on a PCB would render this problem too large to model with the finite element or FDTD method, however, with faster computers this is less of a limiting factor. Specifically, the challenge for differential equation-based methods such as FEM and FDTD is related to the necessity to grid the problem up over a volume. Having both large- and small-scale geometries can then lead to a very large number of unknowns in the numerical solution. The small-scale aspect of the problem is dominated by the *25 mil.* wide trace, and the *45 mil.*, or less, thickness of the substrate. In order to adequately model these features, the grid must be at least on the order of this dimension and preferably smaller. On the other end of the scale spectrum, the effective radiating conductors have a longest dimension of *18 cm*. Gridding up the computational domain with elements dictated by the smallest features can lead to a very large

problem. Among the tremendous advantages of the FEM method is the capability for varying the cell dimensions over the computational domain. The mesh can be made very fine near small features, and expanded to be coarser for the larger features. The FDTD method on the other hand uses a single grid size throughout the computational domain, however, since it is a time-domain method, results over a wide frequency range can be generated with a single simulation. Both a hybrid FEM/MOM and the FDTD method were used to model the present problem of a trace in proximity to a PCB edge.

The FDTD method was first used to model the problem of a trace in proximity to the PCB edge. The board was modeled with cells of dimensions *0.0568 cm* x *0.031 cm* x *0.15 cm.* The dimensions were chosen to model the trace with two elements over its width, and the PCB substrate as two elements thick. The final dimension was chosen to maintain a maximum ratio of 5:1 between any two dimensions. This upper bound on the cell aspect ratio has been determined from experience with FDTD modeling and comparison with measurements on many different types of EMI modeling problems, and is also widely accepted within the numerical modeling community as a general maxim. The outer shield of the semi-rigid coaxial cable was modeled as a flat PEC four cells wide so the width of the flat PEC was close to the equivalent radius of a cylinder. The PCB trace was terminated with a matched load in all simulations. The load was modeled with a lumped element resistor in the substrate at the terminated end of the line. A thin wire connected the end of the signal trace to the PCB reference plane. The PCB substrate was modeled as a dielectric with relative permittivity ε_r=*4.5*. The monopole probe was modeled using a thin-wire algorithm [11], and it was terminated in a lumped *50 Ω* load at the base to model the network analyzer impedance [12]. The magnetic field components circling the resistive termination were modeled using the thin-wire algorithm as well to give the termination the same effective dimensions as the wire. The computational domain was truncated with perfectly matched layers (PML) [13], 8 cells deep, and there were 6 cells of white space between the PCB and monopole geometry and the PMLs. Overall, the computational domain was 109 x 339 x 148 cells, for approximately 5.5 million total cells. The time step was 7.58×10^{-13} *s*. A total of 10,000 time steps were used in the simulations. A sinusoidaly modulated Gaussian source was applied as the trace excitation with frequencies from *100 MHz - 3 GHz*. A Fast Fourier Transform was applied to the time-history to get the frequency domain results.

The FDTD modeled and measured results are compared in Figure 5 for a centered trace, and a trace near the edge with *d = 25 mils*. The agreement between the modeled and measured results is in general good over the entire frequency range. The primary discrepancies are below *1 GHz*. The rate of increase in the sensed electric field compares well between the measured and modeled results on the low-frequency end. However, there is a peak at approximately *1 GHz* in the measured results that is not captured in the modeling.

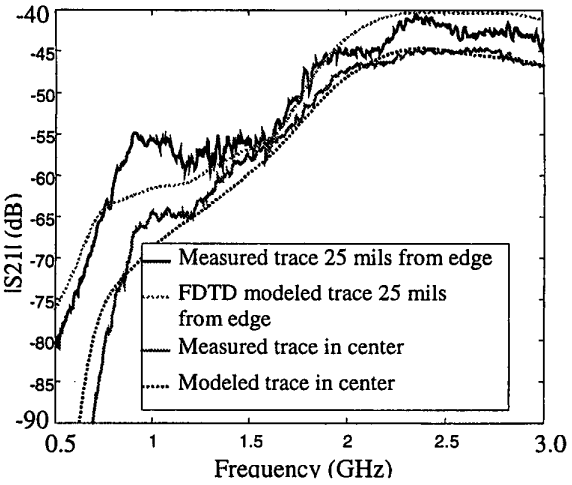

Figure 5: Comparison of FDTD and measured results for a centered trace and a trace near the edge with d = 25 mils.

The test geometry was also modeled using a hybrid FEM/MOM modeling approach [14]. The FEM/MOM modeling approach is particularly well suited for EMI problems because inhomogeneous, small-scale PCB portions of the geometry can be modeled with FEM, and the large scale geometries of the cable can be modeled with MOM. In each case, the specific numerical modeling approach is used where it is particularly suitable, while avoiding portions of the problem for which it is poorly suited. An example of the meshed board with the trace in the center is shown in Figure 6. The mesh was made very fine around the trace where the field geometry varies the most, and becomes much coarser as it approaches the edges of the board.

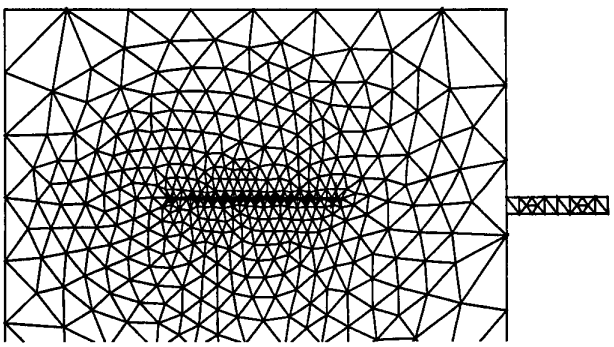

Figure 6: Example of the board mesh for the FEM/MOM hybrid model.

The hybrid modeling approach was used to calculate the common-mode current on the attached cable, and to extract

$|S_{21}|$ from a knowledge of the source voltage and common-mode current [14]. The calculated $|S_{21}|$ was compared to the experimental results as shown in Figure 7. The agreement between the measured and modeled results is favorable although there is a constant difference of nearly *3 dB* over most of the modeled curve.

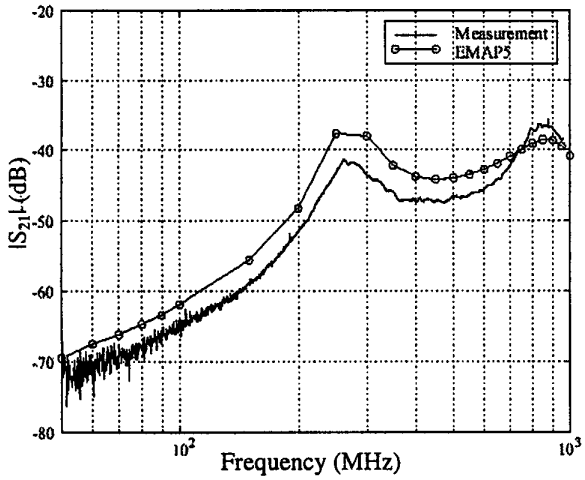

Figure 7: FEM/MOM hybrid modeling and experimental results for a centered trace.

FDTD modeling was also used to evaluate the variation in the near electric-field radiation for different cases of trace height above the signal return plane and proximity to the edge. Computed results for three different trace heights with the trace centered on the return plane, and two different heights for the trace edge *25 mils.* away from the PCB edge are shown in Figure 8. For the centered trace, the increase in $|S_{21}|$ is nearly *6 dB* as the trace height is doubled, indicating that the radiation is directly proportional to the height of the trace over the ground plane. This is consistent with other reported results at lower frequencies [2], [7]. For the trace near the PCB edge, the increase in the radiation as the trace height increases is lower for the two cases shown, approximately *3.5 dB* over the considered frequency range. At frequencies above *1 GHz*, where the trace is no longer electrically short, there are only a few decibels of difference between the centered trace, and the trace near the PCB edge. At lower frequencies, however, there is a significant difference.

As the trace height above the return plane is changed, the characteristic impedance of the line changes as well. In order to compare the results for all cases the termination was changed for each line to make it matched. The characteristic impedance for the trace *22 mils.*, *45 mils.* and, *90 mils.* above the ground plane was *60 Ω*, *90 Ω*, and *116 Ω* respectively. The PCB and trace geometry were modeled in an identical fashion so there were no other variations in the simulations.

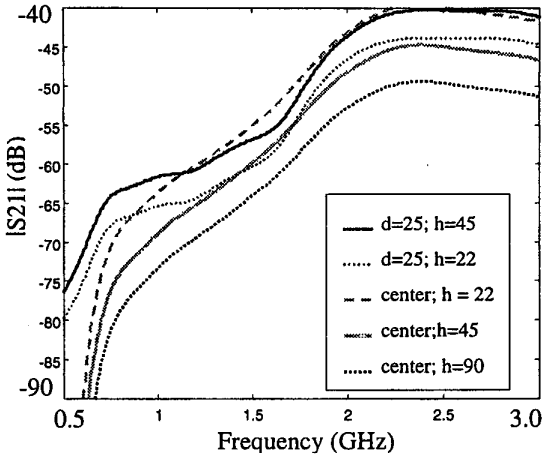

Figure 8: Comparison of the near-electric field radiation for different trace heights above the reference plane for a centered trace, and trace 25 mils from edge.

The agreement of the measured and modeled results demonstrate that numerical modeling is suitable for developing design guidelines regarding trace routing in proximity to PCB edges as a function of the height of the trace above the signal return plane, and the distance of the trace from the PCB edge. The modeled results in Figure 5 for a centered trace are consistent with previously reported results indicating an EMI coupling path dominated by the magnetic field wrapping the reference plane. However, for traces near the PCB edge, the increase in radiation is not consistent with a coupling mechanism dominated by the magnetic field, and further work is needed to understand the relevant physics.

4. CONCLUSIONS

An increase in EMI resulting from a trace containing high-frequency spectral components on it in proximty to a PCB edge was considered. The EMI coupling was investigated both experimentally and through numerical modeling. At low frequencies, the functional variation of the EMI with frequency was consistent with a coupling mechanism dominated by the magnetic field, however, at higher frequencies, the dominant coupling mecahanism(s) was unclear and requires further work. FDTD and FEM/MOM modeling were used, in addition to measurements. In general, the modeled results agreed favorably with the measurements, demonstrating that full-wave numerical modeling provides a good basis for continued investigation of EMI coupling mechanisms for trace near PCB edges, and development of design guidelines.

REFERENCES

[1] A. E. Ruehli, "Inductance calculations in a complex integrated circuit environment", *IBM Journal of Research and Development*, vol. 16, pp. 470-481, 1972.

[2] F. B. M. van Horck, *Electromagnetic Compatibility and Printed Circuit Boards*, Technische Universiteit Eindhoven, 1998.

[3] D. M. Hockanson, J. L. Drewniak, T. H. Hubing, T. P. Van Doren, Fei Sha, C. W.Lam, and L. Rubin, "Quantifying EMI noise sources resulting from finite impedance reference planes", *IEEE Transactions on Electromagnetic Compatibility*, pp. 286-297, November 1997

[4] C. L. Holloway and E. F. Kuester, "Net and partial inductance of a microstrip ground plane", *IEEE Transactions on Electromagnetic Compatibility*, pp. 33-46, February 1998.

[5] C. L. Holloway and G. A. Hufford, "Internal inductance and conductor losses associated with ground plane of a microstrip line", *IEEE Transactions on Electromagnetic Compatibility*, pp. 73-78, May 1997.

[6] F. B. J. Leferink and M. J. C. M. van Doorn, "Inductance of printed circuit board ground planes", *IEEE International Symposium on Electromagnetic Compatibility*, Dallas, TX, 1993, pp. 327-329.

[7] D. M. Hockanson, J. L. Drewniak, T. H. Hubing, T. P. Van Doren, Fei Sha, and M. Wilhelm, "Investigation of fundamental EMI source mechanims driving common-mode radiation from printed circuit boards with attached cables", *IEEE Transactions on Electromagnetic Compatibility*, pp. 557-566, November 1996.

[8] C. L. Holloway and E. F. Kuester, "Closed form expressions for the current density on the ground plane of a microstrip line, with applications to ground plane loss", *IEEE Transactions on Microwave Theory Tech.*, pp. 1204-1207, May 1995.

[9] T. H. Ooi, S. Y. Tan, and H Li, "Study of radiated emissions from pcb with narrow ground plane," *IEEE International Symposium on Electromagnetic Compatibility*, Tokyo, Japan, May 1999, pp. 552-555.

[10] E. C. Jordan, K. G. Balmain, *Electromagneti Waves and Radiating Systems*, Prentice-Hall, Inc., Englewood Cliffs, New Jersey, 1968.

[11] A. Taflove, "The Thin Wire", *Chapter 10 in Computational Electrodynamics: The finite-difference time-domain method*, Artech House Publishers, Boston·London, 1995.

[12] M. Piket-May, A. Taflove, J. Baron, "FDTD modeling of digital signal propagation in 3-D circuits with passive and active loads", *IEEE Trans. Micro. Theory Tech.*, vol. 42, pp 1514-1523, August, 1994.

[13] J. P. Berenger, "Perfectly matched layer for the absorption of electromagnetic waves," *J. Comput. Phys.*, vol. 114, pp 185-200, Oct., 1994.

[14] M. Ali, T.H. Hubing, J. L. Drewniak, "A hybrid FEM/MoM technique for electromagnetic scattering and radition from dielectric objects with attached wires", *IEEE Transactions on Electromagnetic Compatibility*. v 39, Nov 1997, pp304-314.